ACS Sustainable Chemistry & Engineering

pubs.acs.org/journal/ascecg

Research Article

Catechol Patterned Film Enables the Enzymatic Detection of Glucose with Cell Phone Imaging

Si Wu, John R. Rzasa, Eunkyoung Kim, Zhiling Zhao, Jinyang Li, William E. Bentley, Nadine N. Payne, Xiaowen Shi,* and Gregory F. Payne*

Cite This: *ACS Sustainable Chem. Eng.* 2021, 9, 14836−14845

Read Online

ACCESS | Metrics & More | Article Recommendations | Supporting Information

ABSTRACT: Biology provides an array of materials and mechanisms to create sustainable high-performance materials. Here, we prepared a polysaccharide film and patterned it with redox-active catechol moieties using a biomimetic oxidative grafting method. In this proof-of-concept study, we show that the film allows results from an enzymatic biosensing reaction to be reported through cell phone imaging for the detection of glucose in food and beverage products (glucose is a marker for high-fructose corn syrup; HFCS). This method uses glucose dehydrogenase (GDH) to confer molecular recognition, while the NADH product transfers its electrons to catechol moieties that are patterned onto a polysaccharide film. The "accumulation" of electrons by the catechol pattern can be detected because the oxidized quinone state is darker in color than the reduced catechol state. Using a commercially available cell phone imaging app, we demonstrate that HFCS-containing products can be distinguished from analogous products containing either sucrose or artificial sweeteners. Thus, we envision that this method could allow buyers or consumers to detect glucose on-site or in-home. In addition, this work further illustrates the potential of catechol-based materials for performing redox-based functions.

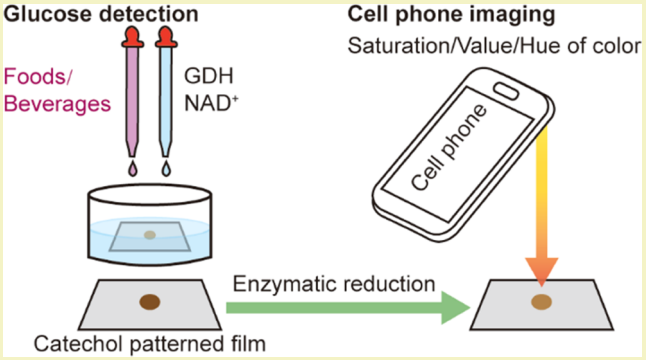

KEYWORDS: *chitosan, catechols, redox, glucose dehydrogenase, high-fructose corn syrup (HFCS), cell phone imaging*

INTRODUCTION

Polysaccharides are sustainable platform materials because they can often be obtained from renewable resources and are generally nontoxic, biocompatible, and biodegradable.[1−3] In addition, many polysaccharides also offer high-performance attributes as they are stimuli-responsive and can reversibly self-assemble to form hydrogel networks in response to various environmental cues (e.g., chitosan is pH-responsive, agarose is thermally responsive, and alginate is calcium-responsive).[4−8] These characteristics confer exciting dynamic properties to polysaccharide-based materials, enabling them to self-heal[9,10] and reconfigure,[11,12] as well as to perform shape memory functions.[13−15]

Previously, we prepared a dual-responsive hydrogel "medium" from an interpenetrating network of chitosan and agarose and showed that an electrode "pen" could write information to this medium.[16−18] In an initial study, we used the electrode pen to write patterns to the medium by imposing cathodic signals to generate spatially localized pH gradients that induced chitosan chains in those regions to self-assemble. We showed that the regions that had been written by electrode patterning had differences in macromolecular structure, as well as differences in physical, chemical, and biological properties.[16] Thus, this electrode patterning enabled the polysaccharide medium to be spatially patterned with both structural and functional information. In this initial study, the structure induced by electrode patterning was reversible and thus the information could be erased from the medium.

More recently, we used the electrode to anodically oxidize catechols to generate reactive *o*-quinones that can undergo irreversible grafting to the chitosan-based polysaccharide medium presumably forming Schiff base and Michael-type adduct linkages (Scheme 1a).[19−21] This anodic writing is simple and rapid and mimics biology's use of enzymatic phenol oxidation for materials fabrication (e.g., to cross-link the mussel's adhesive protein or to sclerotize the insect's cuticle).[22−24] Previous studies have shown that electrode patterning with catechol confers redox activity to the polysaccharide medium, with the catechol patterned regions offering unique molecular electronic properties.[25−28] Specifically, the grafted catechol moieties have two stable molecular

Received: July 20, 2021
Revised: October 9, 2021
Published: October 25, 2021

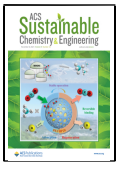

Scheme 1. Catechol Patterned Film to Transduce Enzyme-Generated Signals into Readily Measurable Optical Measurement; (a) Fabrication of Catechol Patterned Chit^0/Agarose Hydrogel Film; (b) Molecular Recognition and Signal Transduction for Glucose Detection Using the Glucose Dehydrogenase (GDH) Enzyme; (c) Measurement after Incubation Using Optical Absorbance Meter and Cell Phone Imaging

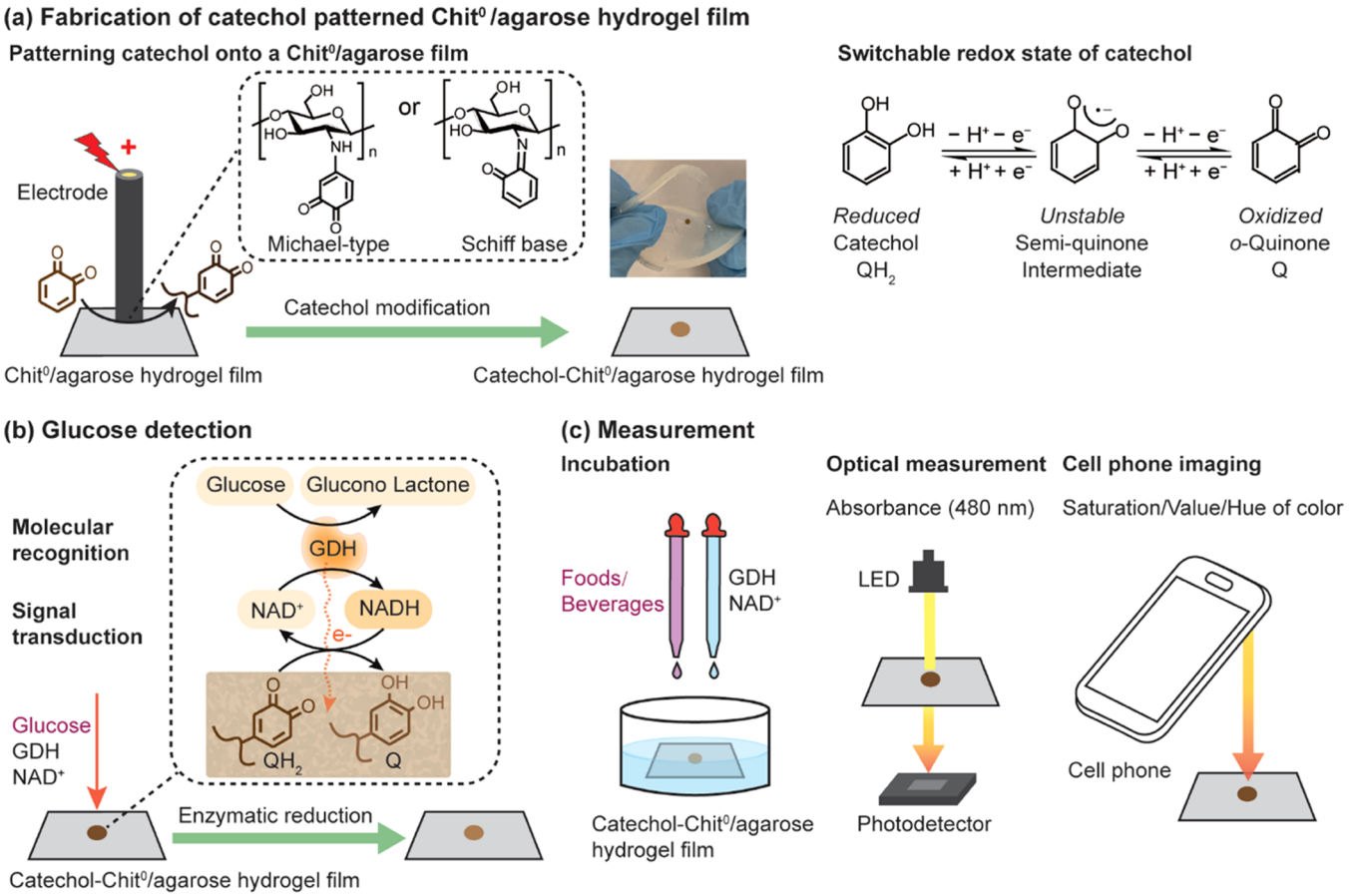

memory states: oxidized (Q) and reduced (QH_2). Importantly, the catechol patterned regions are nonconducting and thus diffusible oxidants or reductants are required to switch catechol's redox memory states.[29−32] Also important is that the redox state of a patterned catechol region can be readily observed visually because the oxidized state has a darker color and higher absorbance at 480 nm.[17,25]

Here, we provide a proof-of-concept illustration for the potential of catechol patterned polysaccharide matrix to be a sustainable medium for portable enzymatic biosensing. The specific example is the detection of glucose as a marker for the adulteration of food and beverage products with lower-cost sweeteners based on high-fructose corn syrup (HFCS).[33] Typically, enzyme biosensors must perform two functions. First, the biosensor must selectively "recognize" the analyte of interest (i.e., glucose) and this molecular recognition function is often performed using an enzyme. Second, the recognition event must be transduced into a measurable signal and often signal transduction schemes for portable biosensors enlist dyes or nanoparticles of uncertain environmental fates.[34−37] Scheme 1b illustrates our approach for coupling the molecular recognition capabilities of the enzyme glucose dehydrogenase (GDH) with the signal transduction capabilities of the catechol patterned film. In this example, a sample suspected of containing glucose is mixed with GDH and NAD^+. If glucose is present: GDH catalyzes the reduction of NAD^+ to NADH; NADH is reoxidized through a redox-cycling reaction with the film; and the redox-cycling reaction converts the film's oxidized Q moieties into their reduced QH_2 state.[38] As illustrated in Scheme 1c, we fabricated our film with a simple catechol pattern (a 2 mm dot) that allows both easy cell phone imaging and convenient visual illustration. Specifically, a change in the redox state of a patterned catechol region can be measured optically by a change in absorbance at 480 nm[17,25] or, as reported here, by cell phone imaging.[17,25,39,40] Compared to other sophisticated approaches (mass spectrometry, chromatography, etc.) that detect nonsucrose sweeteners, our method is simple, cost-effective, time-saving, portable, and sustainable. We envision that this method may allow buyers or consumers to detect glucose in adulterated raw materials or products in near-real-time on-site or in-home.[41−44]

MATERIALS AND METHODS

Materials. Chitosan, agarose, catechol, 1,1′-ferrocene dimethanol (Fc), D-(+)-glucose, D-(−)-fructose, sucrose, glucose dehydrogenase (GDH) from *Pseudomonas* sp., and *β*-nicotinamide adenine dinucleotide sodium salt (NAD^+) were purchased from Sigma-Aldrich. All reagents were used as received without further purification. The water (>18 MΩ) used in this study was obtained from a Super-Q water system (Millipore). The solutions of mediator were prepared in phosphate buffer (0.1 M; pH 7.0).

Fabrication of Chit^0/Agarose Film. A chitosan solution was prepared by dissolving chitosan (3% w/v) with stoichiometric amounts of hydrochloric acid (final pH 5.5). An equal volume of this acidic chitosan solution was mixed with a warm agarose solution

https://doi.org/10.1021/acssuschemeng.1c04896
ACS Sustainable Chem. Eng. 2021, 9, 14836−14845

(2% w/v; 70 °C) to form a warm, slightly acidic blend (1.5% chitosan, 1% agarose). The blended solution (about 3 grams) was poured into a transparent Petri dish and then cooled to room temperature to form the agarose hydrogel network (2 mm thickness). Chitosan (the protonated form is designated Chit-H^+, and the neutral form is designated Chit^0) was neutralized by immersing the Chit-H^+/agarose film in a basic solution (1 M NaOH; 1 h). This film was designated Chit^0/agarose.[14,16,45,46] After that, this hydrogel was rinsed thoroughly with distilled water.

Surface Patterning of Catechol onto a Chit^0/Agarose Film. Catechol moieties were grafted to chitosan (5 mC electrical charge = $\int i dt$, where "i" is current) by immersing the Chit^0/agarose hydrogel in a catechol solution (10 mM catechol in phosphate buffer, pH 7.0), placing a standard gold electrode (2 mm diameter) directly above the film (we estimate the electrode film distance to be less than 30 μm), imposing an oxidizing voltage (+0.6 V vs Ag/AgCl) input. Electrochemical fabrication contains three electrodes: a standard gold working electrode (2 mm diameter), a platinum wire counter electrode, and a Ag/AgCl reference electrode (CH Instruments 420A electrochemical analyzer). After modification, the catechol patterned hydrogel film was washed thoroughly with phosphate buffer.

Optical Absorbance Meter Measurement. A custom scanning optical absorbance meter was constructed for this project that allows for the automatic measurement of optical transmittance (and thereby absorbance) as a function of linear position through the sample. The system consists of the following components: a 480 nm light-emitting diode (LED) light source (CREE C503B-BCS-CV0Z0461) fixed in a driver mount (Thorlabs LEDMT1F). The outgoing beam is shaped by an adjustable iris (Thorlabs SM1D12CZ) to ensure that the beam size is not larger than the sample in question. After passing through the sample, the transmitted light is filtered by a narrow-band interference filter (Thorlabs FB480−10) and then detected and amplified by a photodetector module (Thorlabs PDA100A2). This signal is then digitized by an Arduino UNO microcontroller platform that has a 12-bit resolution ADC ranging over 0−5 V.

The sample is moved through the light beam with a linear servo actuator (Thorlabs KMTS50E, maximum velocity 2.4 mm/s), which is controlled by a custom Windows GUI written in C#. This GUI also controls the Arduino, syncing the position and absorbance measurements in time. Prior to moving through the sample, the GUI records a baseline signal, which is then used to calculate the absorbance.[17] All data are saved as.csv text files, and the results are also displayed in real time on the screen.

Cell Phone Imaging. The cell phone-based measurement was performed by a color analyzing application (Live Color, available on App Store) that automatically quantifies images of each spot in terms of three signals: Saturation (S), Value (V), and Hue (H).

RESULTS AND DISCUSSION

Catechol Patterned Film Enables Enzymatic Detection of Glucose. As illustrated in Scheme 1a, we extended a simple electrofabrication method[32,47−51] to pattern catechols onto the surface of chitosan/agarose hydrogel film.[17,18,25] The films were first prepared by mixing warm agarose and slightly acidic chitosan solutions, casting these solutions into films, and then neutralizing the protonated chitosan chains (Chit-H^+) into their deprotonated state (Chit^0). This film was designated Chit^0/agarose.[14,16,45,46] The spatially selective patterning of the Chit^0/agarose film with catechol moieties was performed by immersing the film in a catechol solution (10 mM), placing a standard gold electrode (2 mm diameter) directly above the film surface (we estimate the electrode film distance to be less than 30 μm), and applying an oxidizing voltage (+0.6 V vs Ag/AgCl). At this voltage, catechols are anodically oxidized to reactive o-quinones that can graft to chitosan through putative Schiff base linkages and Michael-type adducts. After modification, the catechol patterned hydrogel film was washed thoroughly with phosphate buffer.

Previous studies have shown that the grafted catechol moieties are redox-active and can be repeatedly switched between their oxidized and reduced states. However, these films are nonconducting and thus switching catechol's redox state requires diffusible oxidants or reductants.[29−32] Scheme 2 illustrates the electrochemical method used to set the patterned catechols to their oxidized state by immersing the catechol-Chit^0/agarose hydrogel film in a solution containing the mediator ferrocene dimethanol (Fc; E^0 = +0.25 V), placing an electrode above the patterned catechol region of the film, and imposing an oxidizing voltage (+0.5 V, 15 min). This method induces an oxidative redox-cycling mechanism in which Fc mediates the transfer of electrons to the electrode by converting the reduced catechol moieties (QH_2) into their oxidized o-quinones (Q).

Scheme 2. Setting Catechol Pattern to Oxidized State

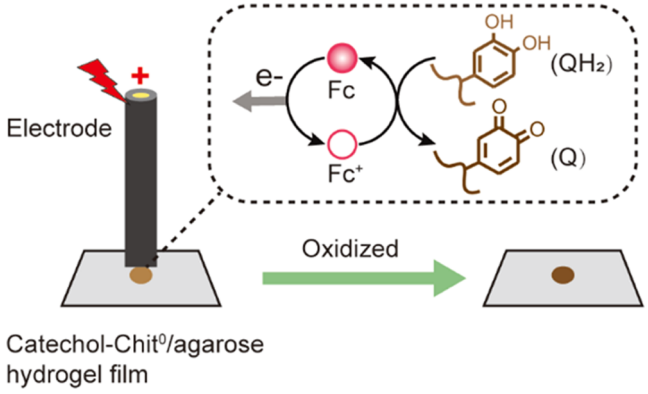

Optical Absorbance Meter Measurement. We first demonstrated the glucose detection mechanism illustrated in Scheme 1b. Experimentally, we immersed an oxidized catechol-Chit^0/agarose hydrogel film in a solution containing glucose (10 mM), GDH (10 U/mL), and NAD^+ (2.5 μM) and monitored changes in optical absorbance using a fixed-wavelength (480 nm) custom-built optical absorbance meter as illustrated in Figure 1a. The inset plot in Figure 1b shows that the absorbance for this experimental film decreases over the 30 min measurement period. This absorbance decrease is consistent with the conversion of the film's catechol moieties from their oxidized Q state to their reduced QH_2 state. The inset plot also shows results for several control films. Two electrochemical controls were prepared using redox-cycling reactions to convert the film catechols to either their oxidized Q or reduced QH_2 states: the oxidized film shows high absorbance; the reduced film shows low absorbance; and the absorbance of both films remains nearly constant over the 30 min measurement period. Three biochemical controls were prepared by incubating an oxidized catechol-Chit^0/agarose hydrogel film in a solution containing only two of the three reaction components: the inset plot in Figure 1b shows that the absorbance is high and remains nearly constant for all of these biochemical controls.

The bar chart in Figure 1b summarizes results from this initial experiment. Specifically, the absorbance difference ($\Delta Absorbance_{30}$) was calculated between the final (t = 30 min) and initial (t = 0 min) measurements ($\Delta M_{30} = (M_0 - M_{30})$, where "$M_0$" is the measurement at 0 min and "M_{30}" is the

https://doi.org/10.1021/acssuschemeng.1c04896
ACS Sustainable Chem. Eng. 2021, 9, 14836−14845

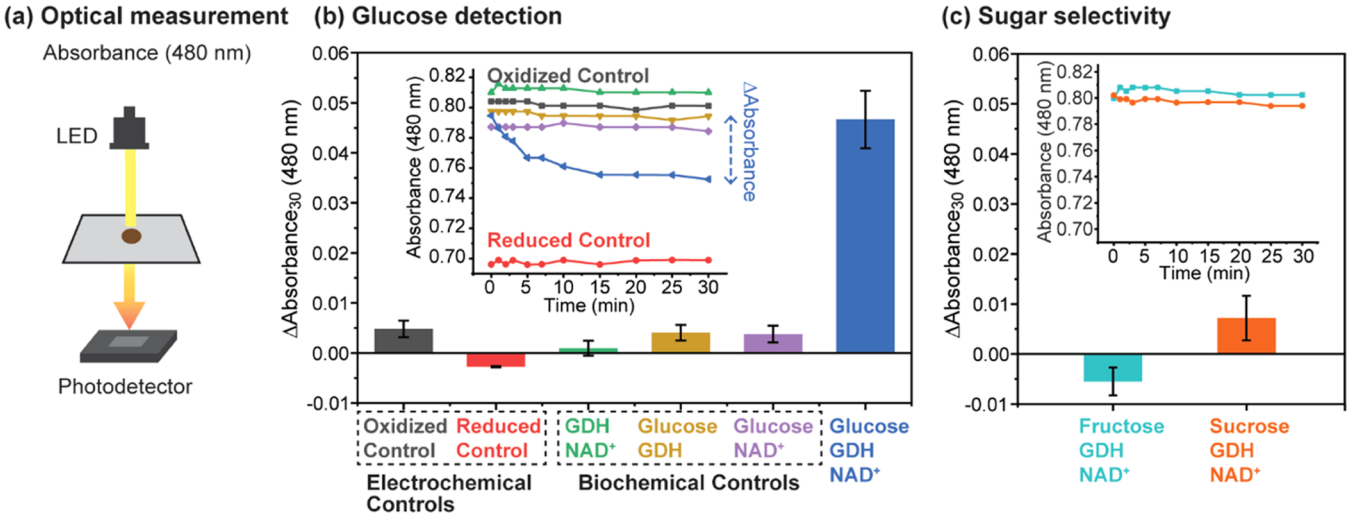

Figure 1. Enzymatic detection of glucose is transduced into an optical signal. (a) Schematic of optical absorbance measurement. (b) Detection of glucose leads to a large change in the optical absorbance ($\Delta Absorbance_{30}$) of the catechol patterned film compared to changes observed with electrochemical and biochemical controls. (c) Enzyme confers sugar selectivity: minimal changes in the $\Delta Absorbance_{30}$ of the catechol patterned film were observed in the presence of nonglucose sugars.

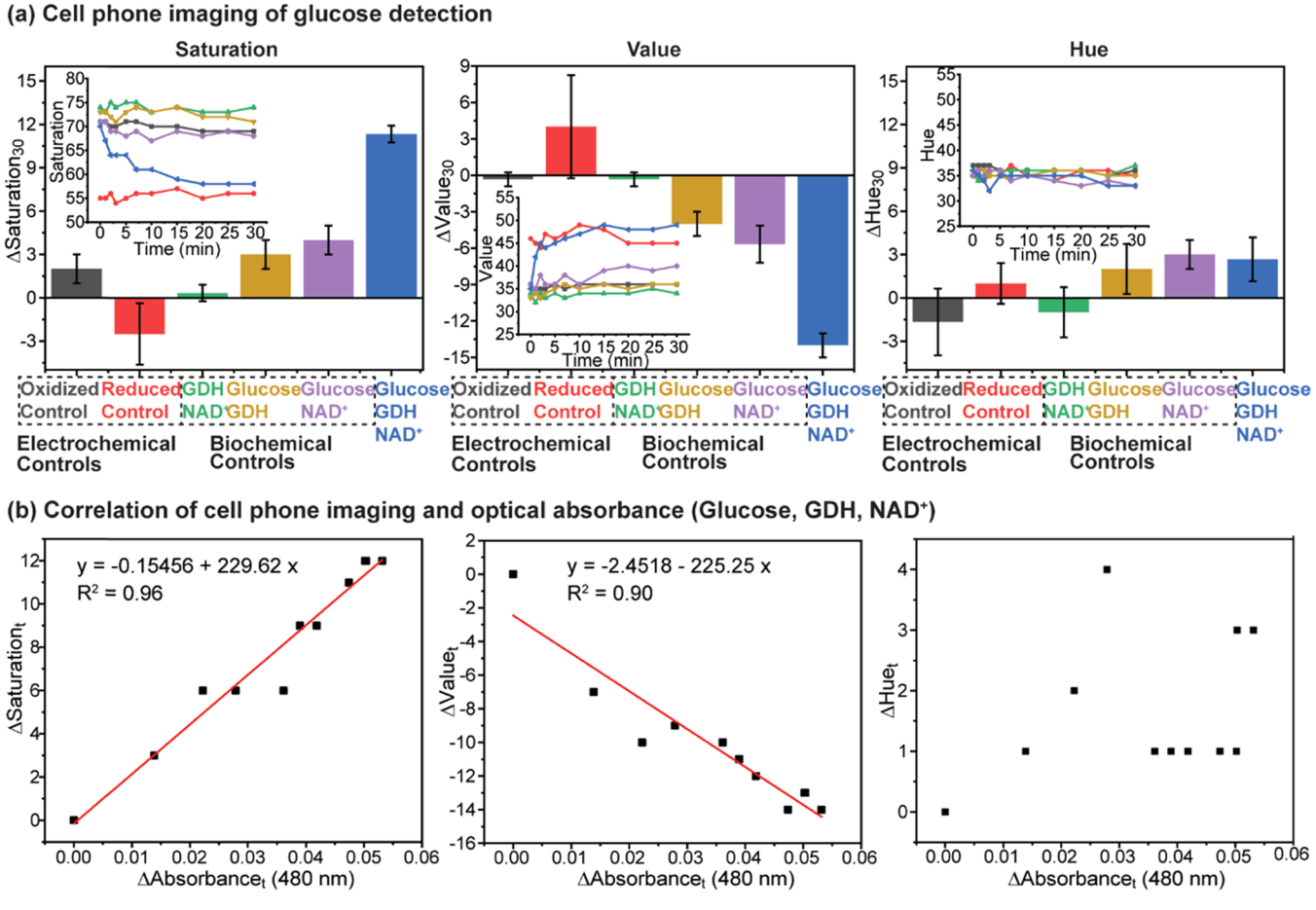

Figure 2. Enzymatic detection of glucose is transduced through cell phone imaging. (a) Detection of glucose leads to a large change in the ΔSaturation and ΔValue (but not ΔHue) signals of the catechol patterned film compared to changes observed with electrochemical and biochemical controls. (b) Correlation of cell phone imaging and optical absorbance measurements for incubation in the presence of glucose, GDH, and NAD^+.

measurement at 30 min). This bar chart shows that a large absorbance difference was observed for the experimental film, while small differences were observed for the two electrochemical controls and three biochemical controls. These results are consistent with the mechanism proposed in Scheme 1b and indicate that the catechol-$Chit^0$/agarose hydrogel film

https://doi.org/10.1021/acssuschemeng.1c04896
ACS Sustainable Chem. Eng. 2021, 9, 14836−14845

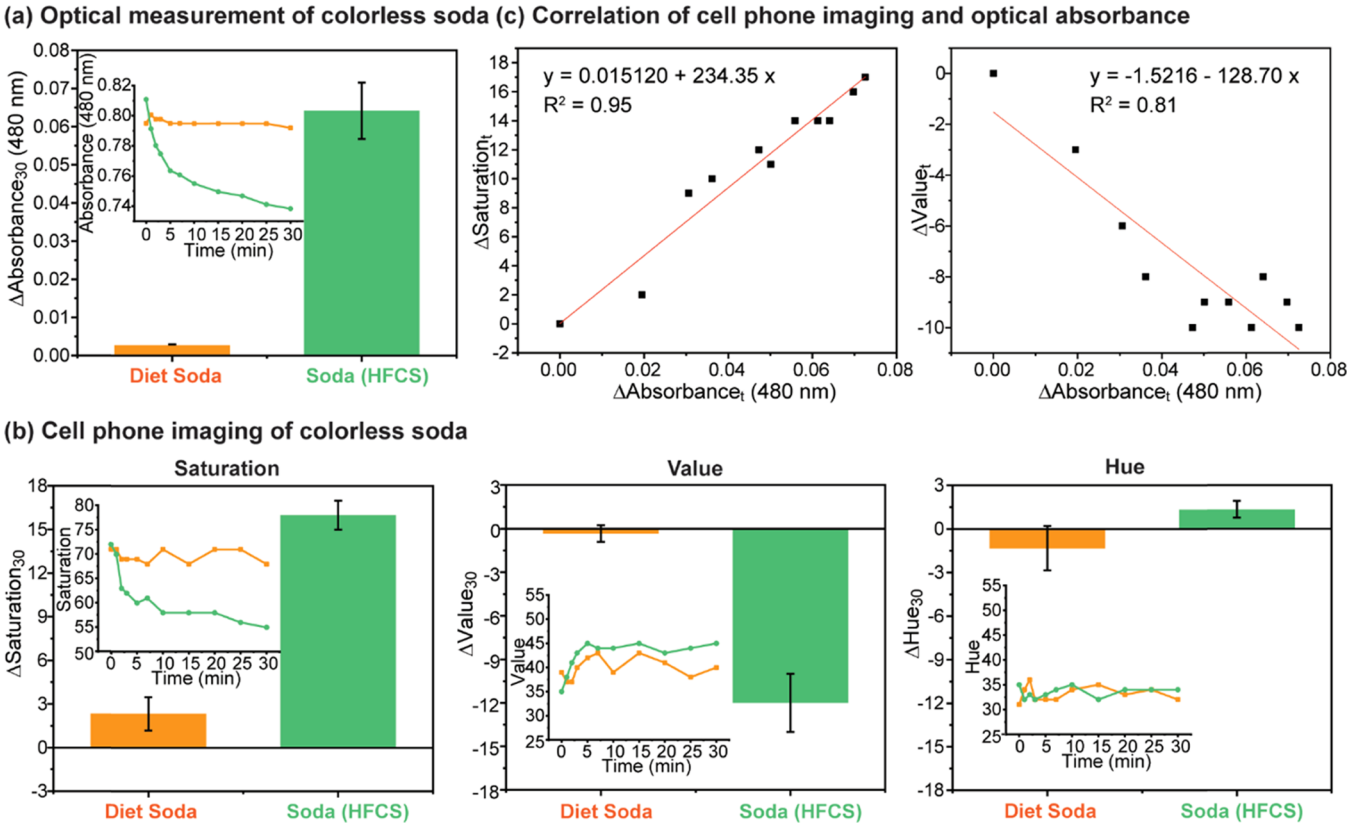

Figure 3. Enzymatic detection of glucose in colorless soda beverages. Glucose-containing soda and a diet version of the same brand were compared by observing the optical changes of a catechol patterned film using: (a) optical absorbance meter and (b) cell phone. (c) Correlation of the cell phone imaging and optical absorbance measurements for the detection of glucose in colorless soda beverages.

can transduce enzyme-generated signals into readily measurable optical outputs.

Next, we demonstrated the sugar selectivity of glucose detection by immersing an oxidized catechol-Chit^0/agarose hydrogel film in a solution containing fructose or sucrose (10 mM), GDH (10 U/mL) and NAD$^+$ (2.5 μM), incubating for 30 min and monitoring optical absorbance. The inset plot in Figure 1c shows the absorbance of fructose control and sucrose control remain at a high level. The bar chart in Figure 1c shows small optical absorbance differences (ΔAbsorbance$_{30}$) in the presence of fructose or sucrose. The results illustrate that neither fructose nor sucrose can be oxidized by this enzymatic reaction.

Cell Phone Imaging Measurement. Since the catechol film can transduce the detection of glucose into a change in color, we next examined whether these optical changes could be detected from a cell phone image.[35,52,53] The cell phone imaging measurement was performed by a color analyzing application (Live Color, available on App Store) that automatically quantifies images of each spot in terms of three signals: Saturation (S) refers to the brilliance and intensity of a color and ranges from 0% (no color that is a shade of gray) to 100% (saturated color); Value (V) quantifies lightness or darkness and ranges from 0% (black) to 100% (white); and Hue (H) is defined as the degree to which a stimulus can be described as similar to or different from stimuli that are described as red, green, blue, and yellow. It ranges from 0 to 360°, and each value corresponds to a color such as 0° is red, 60° is yellow, 120° is green, and 240° is blue.

To test whether cell phone imaging could be used to detect the change in the catechol film's redox state, we performed a similar experiment to that in Figure 1 except we used the cell phone to generate images that were subsequently analyzed. The left inset curve in Figure 2a shows that the Saturation signal for the experimental film decreased over the 30 min measurement period, which is consistent with the conversion of an initially oxidized Q state of catechol moieties into their reduced QH_2 state. Results for the two electrochemical controls show a high Saturation for the oxidized control, a low Saturation for the reduced control, and the Saturation values for these controls remained nearly constant during the measurement period. Results for the three biochemical controls show high and relatively stable Saturation values consistent with an oxidized film that is not undergoing a change in redox state. The bar chart in Figure 2a (left) summarizes these results and shows the Saturation difference (ΔSaturation$_{30}$), which was calculated between the final (t = 30 min) and initial (t = 0 min) measurements. This bar chart shows that a large Saturation difference was observed for the experimental film, while small differences were observed for the two electrochemical controls and the three biochemical controls.

The middle inset curve in Figure 2a shows results for a second imaging signal, Value. Results for the experimental film show the Value increased during incubation time consistent with the catechol film undergoing a change in redox state. Results for the two electrochemical controls show that: the oxidized control had a low Value, the reduced control had a high Value, and the Value for these controls remained

https://doi.org/10.1021/acssuschemeng.1c04896
ACS Sustainable Chem. Eng. 2021, 9, 14836−14845

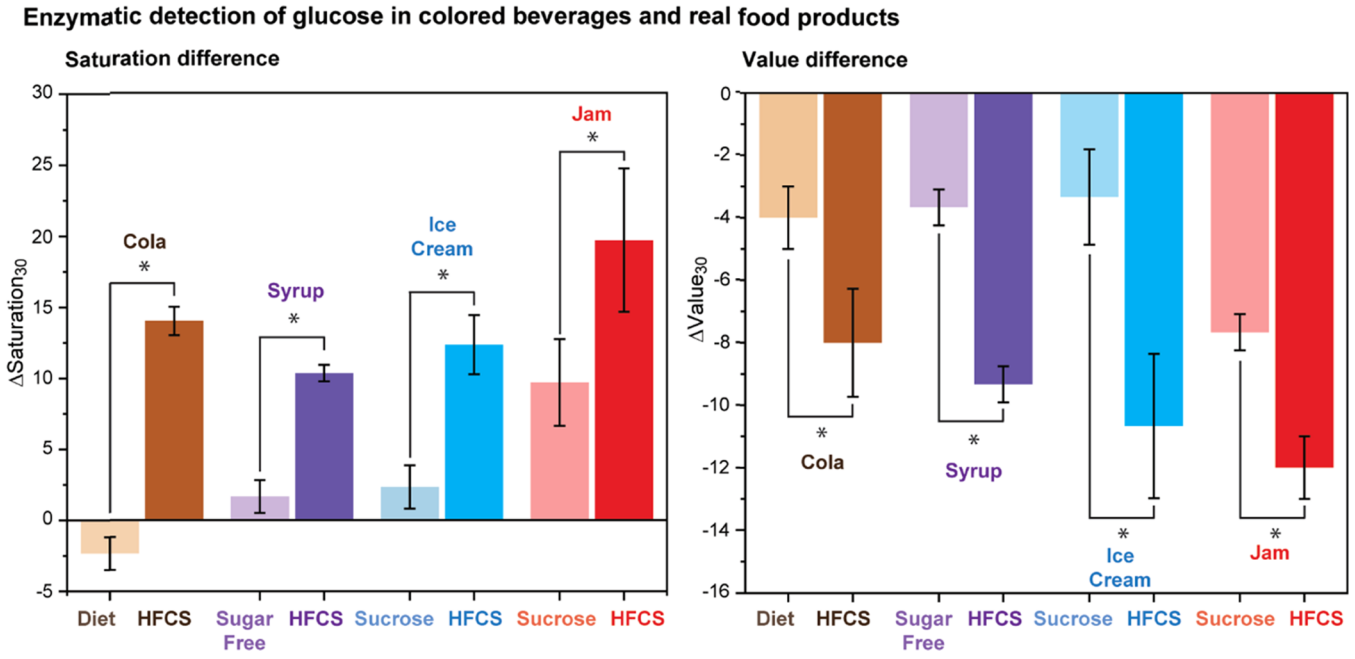

Figure 4. Enzymatic detection of glucose in colored beverages and real food products. A glucose-containing sample and a diet or sucrose-containing version of the same or a similar brand were compared by observing the ΔSaturation and ΔValue values of a catechol patterned film using a simple cell phone imaging measurement (* near the bar indicates a significant difference, $p < 0.05$).

relatively stable during the measurement period. Results for the three biochemical controls show that: these controls had low and nearly stable Values consistent with an oxidized catechol film that did not change redox state. The bar chart in Figure 2a (middle) summarizes these results and shows the Value difference ($\Delta Value_{30}$), which was calculated between the final and initial measurements. The bar chart shows that during incubation, the experimental film underwent a comparatively large change in Value, while relatively small Value differences were observed for the two electrochemical controls and the three biochemical controls.

The inset curve and bar graph in Figure 2a (right) show results for the third imaging signal, Hue. As shown, minimal changes in Hue were observed for the experimental film, the two electrochemical controls, and the three biochemical controls. Thus, the Hue signal appears to be less sensitive to changes in catechol's redox state compared to either the Saturation or Value signals.

We next tested the cell phone imaging to ensure that we could discern the sugar specificity associated with enzymatic glucose detection. Figure S1 in the Supporting Information shows minimal changes in Saturation, Value, and Hue in the presence of fructose or sucrose. Thus, as expected, there were no significant changes in the cell phone imaging signals when a nonglucose sugar was tested.

The correlations between the cell phone imaging and more-standard (but less convenient) optical absorbance measurements for the experimental sample (containing glucose, GDH, and NAD^+) are summarized in Figure 2b. Specifically, we calculated ΔM_t as the difference between different time interval and initial measurement ($\Delta M_t = (M_0 - M_t)$, where "M_t" is the measurement at time, t). These plots show a positive correlation between the Saturation difference ($\Delta Saturation_t$) and the Absorbance difference ($\Delta Absorbance_t$), a negative correlation between the Value difference ($\Delta Value_t$) and the Absorbance difference ($\Delta Absorbance_t$), and no correlation between the Hue difference (ΔHue_t) and the Absorbance difference ($\Delta Absorbance_t$).

Overall, the results in Figure 2 show that changes in the redox state of the catechol pattern can transduce results from the enzymatic detection of glucose into optical signals that are measurable using convenient cell phone applications.

Enzymatic Detection of Glucose in Real Samples. To illustrate the potential for applying the catechol film for the detection of glucose in real samples, we first considered an example of a colorless beverage. In this example, we compared the analysis of a colorless regular soda containing high-fructose corn syrup (HFCS) with the diet version of the same brand. Experimentally, we mixed the soda (diluted in half) with GDH (10 U/mL) and NAD^+ (2.5 μM), immersed an oxidized catechol-$Chit^0$/agarose hydrogel film in this mixture, and monitored the optical absorbance. The inset curve in Figure 3a shows that when the film was incubated with glucose-containing soda, the absorbance of the catechol patterned film decreased during the 30 min measurement period. In contrast, the absorbance for the catechol pattern did not change when the film was incubated with the diet version of the soda. The bar graph in Figure 3a summarizes these results showing a large absorbance difference ($\Delta Absorbance_{30}$) for the catechol film incubated with the glucose-containing (but not diet) soda. These results indicate that the change in optical absorbance associated with the catechol pattern's redox state could be used to detect the presence of glucose in colorless soda.

We next examined the ability of the simple cell phone imaging to detect glucose by immersing an oxidized catechol-$Chit^0$/agarose hydrogel film in a solution containing regular or diet soda (diluted in half) with GDH (10 U/mL) and NAD^+ (2.5 μM); generating cell phone images; and analyzing the Saturation, Value, and Hue signals of the catechol patterned film. The inset curve and bar graph in Figure 3b (left) show that the Saturation signal decreased over the 30 min period

https://doi.org/10.1021/acssuschemeng.1c04896
ACS Sustainable Chem. Eng. 2021, 9, 14836−14845

when the catechol patterned film was incubated with the glucose-containing soda, while the Saturation signal remained nearly constant for the catechol patterned film incubated with the diet soda. The inset curve and bar graph in Figure 3b (middle) shows that the Value signal increased over the 30 min period when the catechol patterned film was incubated with the glucose-containing soda, while the Value signal was relatively stable during incubation with the diet soda. The inset curve and bar graph in Figure 3b (right) shows that the Hue signal does not change during incubation with either regular or diet soda.

The correlation between the cell phone imaging and optical absorbance measurements for the detection of glucose in colorless beverages is summarized in Figure 3c. As shown, there is a positive correlation between the Saturation difference ($\Delta Saturation_t$) and the Absorbance difference ($\Delta Absorbance_t$), and a negative correlation between the Value difference ($\Delta Value_t$) and the Absorbance difference ($\Delta Absorbance_t$). For the correlation with $\Delta Saturation_t$, it is interesting to note that there is good agreement of the slopes between measurements with the colorless beverage and those with the buffered solutions (Figure 2b). These results indicate that catechol allows coupling of an enzymatic reaction with cell phone imaging for the detection of glucose in a simple food product (e.g., a colorless beverage).

We next examined the ability of cell phone imaging to detect glucose in a dark-colored beverage (an HFCS-containing cola vs the diet version of the same brand) and a liquid food product (an HFCS-containing syrup vs the sugar-free version of the same brand). Experimentally, we immersed an oxidized catechol-$Chit^0$/agarose hydrogel film into a solution containing the beverage or food product (diluted in half), GDH (10 U/mL), and NAD^+ (2.5 μM) and used cell phone imaging to analyze Saturation and Value signals over 30 min incubation period. The first entry in Figure 4 shows that when the film was incubated with glucose-containing cola, the Saturation difference ($\Delta Saturation_{30}$) and Value difference ($\Delta Value_{30}$) of the catechol patterned film were observed to be significantly larger compared to the film incubated with the diet cola (statistical analysis by one-way ANOVA with SPSS 19.0 software). The second entry in Figure 4 shows a significant difference in the catechol patterned film's $\Delta Saturation_{30}$ and $\Delta Value_{30}$ between the glucose-containing syrup group and the sugar-free syrup group.

Finally, we examined whether the catechol film could discern the sugar specificity in nonliquid ice cream and jam products. Experimentally, we prepared 1 g of nonliquid food product, diluted the product in half with phosphate buffer, and mixed with GDH (10 U/mL) and NAD^+ (2.5 μM); immersed an oxidized catechol-$Chit^0$/agarose hydrogel film in the mixed solution; and used cell phone imaging to analyze the Saturation and Value signals over a 30 min incubation period. Results for glucose-containing ice cream in Figure 4 show a significant difference of $\Delta Saturation_{30}$ and $\Delta Value_{30}$ compared to results for sucrose-containing ice cream of a similar product.

In the last example, we tested strawberry jam containing HFCS and a similar product of jam containing sucrose. The last entry in Figure 4 shows that the $\Delta Saturation_{30}$ and $\Delta Value_{30}$ values of the catechol patterned film for each group were observed to be high, which may be caused by the reducing activity (e.g., Vitamin C) in the strawberry jam products. Specifically, jam is known to contain relatively high levels of ascorbate, which is known to be capable of interfering with our measurement (i.e., both ascorbate and the enzyme-generated NADPH are known to donate electrons to switch the redox state of the catechol). Despite this interference, there remains a significant difference of $\Delta Saturation_{30}$ and $\Delta Value_{30}$ for glucose detection between the glucose-containing jam group and the sucrose-containing jam group. Thus, for the detection of products containing interfering components, it may be necessary to perform a control measurement (i.e., without enzyme or NAD^+) to detect interference.

In summary, the results in Figure 4 demonstrate that $\Delta Saturation_{30}$ and $\Delta Value_{30}$ of the catechol patterned film for glucose detection in various beverage and food products could be measured by a simple and rapid cell phone imaging measurement.

CONCLUSIONS

In conclusion, we report the adaptation of an enzymatic glucose assay in which the enzyme's activity (i.e., the generation of NADH) is transduced into a colorimetric signal that can be detected by cell phone imaging. The concept was demonstrated for the discrimination of several food and beverage products containing HFCS compared to analogous products containing sucrose or artificial sweeteners. There are many opportunities to optimize performance for the specific application (glucose detection), for instance, the film thickness, grafting density, pattern shape and size, and uniformity along the thickness might affect sensitivity, selectivity, and response time. Our goal was to provide a proof of concept for sustainable biosensing through bio-based materials and mechanisms (e.g., mechanisms for signal recognition and transduction). We envision that this method could provide a simple means for the on-site or in-home detection of glucose-containing products to allow buyers or consumers to make informed decisions.

In addition, this work illustrates two broader concepts. First, we use biologically derived materials (i.e., the polysaccharides agarose and chitosan) for the fabrication of functional films. Increasingly, bio-derived materials are being investigated for the creation of high-performance materials that are expected to be environmentally friendly, biocompatible, and potentially even edible.[33,54−59] Second, we enlist the unique properties of catechol to report the activities of an enzymatic redox reaction through catechol's redox-state-dependent optical properties. Catechols (including catechols from foods)[38] are gaining importance in functional materials because they have two stable redox states (Q and QH_2) that enable them to serve as bistable switches and molecular memory devices for bioelectronics applications[17,25] and can exchange electrons with common biological oxidants and reductants providing a means to communicate with biology through its native redox modality.[60,61] Thus, controlling the properties of polysaccharide-based materials and the redox reactions of phenolics may be integral not only for functional foods but also for sustainable high-performance materials.

ASSOCIATED CONTENT

Supporting Information

The Supporting Information is available free of charge at https://pubs.acs.org/doi/10.1021/acssuschemeng.1c04896.

Discerning sugar specificity via cell phone imaging and small changes in the $\Delta Saturation_{30}$, $\Delta Value_{30}$, and

https://doi.org/10.1021/acssuschemeng.1c04896
ACS Sustainable Chem. Eng. 2021, 9, 14836−14845

ΔHue_{30} signals observed upon testing nonglucose sugars (Figure S1) (PDF)

AUTHOR INFORMATION

Corresponding Authors

Xiaowen Shi − *School of Resource and Environmental Science, Hubei International Scientific and Technological Cooperation Base of Sustainable Resource and Energy, Hubei Engineering Center of Natural Polymers-Based Medical Materials, Hubei Biomass-Resource Chemistry and Environmental Biotechnology Key Laboratory, Wuhan University, Wuhan 430079, China;* orcid.org/0000-0001-8294-2920; Email: shixw@whu.edu.cn

Gregory F. Payne − *Robert E. Fischell Institute for Biomedical Devices, University of Maryland, College Park, Maryland 20742, United States; Institute for Bioscience and Biotechnology Research, University of Maryland, College Park, Maryland 20742, United States;* orcid.org/0000-0001-6638-9459; Email: gpayne@umd.edu

Authors

Si Wu − *School of Resource and Environmental Science, Hubei International Scientific and Technological Cooperation Base of Sustainable Resource and Energy, Hubei Engineering Center of Natural Polymers-Based Medical Materials, Hubei Biomass-Resource Chemistry and Environmental Biotechnology Key Laboratory, Wuhan University, Wuhan 430079, China; College of Resources and Environmental Engineering, Wuhan University of Science and Technology, Wuhan 430081, China;* orcid.org/0000-0001-6325-3951

John R. Rzasa − *Robert E. Fischell Institute for Biomedical Devices, University of Maryland, College Park, Maryland 20742, United States; Fischell Department of Bioengineering and Research, University of Maryland, College Park, Maryland 20742, United States*

Eunkyoung Kim − *Robert E. Fischell Institute for Biomedical Devices, University of Maryland, College Park, Maryland 20742, United States; Institute for Bioscience and Biotechnology Research, University of Maryland, College Park, Maryland 20742, United States;* orcid.org/0000-0003-2566-4041

Zhiling Zhao − *Robert E. Fischell Institute for Biomedical Devices, University of Maryland, College Park, Maryland 20742, United States; Institute for Bioscience and Biotechnology Research, University of Maryland, College Park, Maryland 20742, United States;* orcid.org/0000-0003-0186-7215

Jinyang Li − *Fischell Department of Bioengineering and Research and Institute for Bioscience and Biotechnology Research, University of Maryland, College Park, Maryland 20742, United States*

William E. Bentley − *Robert E. Fischell Institute for Biomedical Devices, University of Maryland, College Park, Maryland 20742, United States; Fischell Department of Bioengineering and Research and Institute for Bioscience and Biotechnology Research, University of Maryland, College Park, Maryland 20742, United States;* orcid.org/0000-0002-4855-7866

Nadine N. Payne − *Retired, Research and Development, McCormick and Company, Inc., Baltimore, Maryland 21031, United States*

Complete contact information is available at: https://pubs.acs.org/10.1021/acssuschemeng.1c04896

Notes

The authors declare no competing financial interest.

ACKNOWLEDGMENTS

This work was supported by the United States National Science Foundation (ECCS-1807604; CBET-1932963; and CBET-1805274) and Defense Threat Reduction Agency (HDTRA-11910021) and also by the China National Natural Science Foundation of China (22075215), Key Research and Development Program of Hubei Province (2020BCA079), National Key Research and Development Program of China (2019YFE0114400), and the China Scholarship Council.

REFERENCES

(1) Meyers, M. A.; Chen, P. Y.; Lin, A. Y. M.; Seki, Y. Biological Materials: Structure and Mechanical Properties. *Prog. Mater. Sci.* **2008**, *53*, 1−206.

(2) Liu, Z.; Jiao, Y.; Wang, Y.; Zhou, C.; Zhang, Z. Polysaccharides-Based Nanoparticles as Drug Delivery Systems. *Adv. Drug Delivery Rev.* **2008**, *60*, 1650−1662.

(3) Manavitehrani, I.; Fathi, A.; Badr, H.; Daly, S.; Shirazi, A. N.; Dehghani, F. Biomedical Applications of Biodegradable Polyesters. *Polymers* **2016**, *8*, No. 20.

(4) Thambi, T.; Phan, V. H. G.; Lee, D. S. Stimuli-Sensitive Injectable Hydrogels Based on Polysaccharides and Their Biomedical Applications. *Macromol. Rapid Commun.* **2016**, *37*, 1881−1896.

(5) Nordin, N.; Bordonali, L.; Badilita, V.; MacKinnon, N. Spatial and Temporal Control Over Multilayer Bio-Polymer Film Assembly and Composition. *Macromol. Biosci.* **2019**, *19*, No. 1800372.

(6) Gray, K. M.; Liba, B. D.; Wang, Y.; Cheng, Y.; Rubloff, G. W.; Bentley, W. E.; Montembault, A.; Royaud, I.; David, L.; Payne, G. F. Electrodeposition of a Biopolymeric Hydrogel: Potential for One-Step Protein Electroaddressing. *Biomacromolecules* **2012**, *13*, 1181−1189.

(7) Vivcharenko, V.; Benko, A.; Palka, K.; Wojcik, M.; Przekora, A. Elastic and Biodegradable Chitosan/Agarose Film Revealing Slightly Acidic PH for Potential Applications in Regenerative Medicine as Artificial Skin Graft. *Int. J. Biol. Macromol.* **2020**, *164*, 172−183.

(8) Vivcharenko, V.; Wojcik, M.; Przekora, A. Cellular Response to Vitamin C-Enriched Chitosan/Agarose Film with Potential Application as Artificial Skin Substitute for Chronic Wound Treatment. *Cells* **2020**, *9*, No. 1185.

(9) Du, Y.; Yang, F.; Yu, H.; Cheng, Y.; Guo, Y.; Yao, W.; Xie, Y. Fabrication of Novel Self-Healing Edible Coating for Fruits Preservation and Its Performance Maintenance Mechanism. *Food Chem.* **2021**, *351*, No. 129284.

(10) Park, N.; Chae, S. C.; Kim, I. T.; Hur, J. Fabrication of Self-Healable and Patternable Polypyrrole/Agarose Hybrid Hydrogels for Smart Bioelectrodes. *J. Nanosci. Nanotechnol.* **2016**, *16*, 1400−1404.

(11) He, H.; Cao, X.; Dong, H.; Ma, T.; Payne, G. F. Reversible Programing of Soft Matter with Reconfigurable Mechanical Properties. *Adv. Funct. Mater.* **2017**, *27*, No. 1605665.

(12) Tsai, C. C.; Payne, G. F.; Shen, J. Exploring PH-Responsive, Switchable Crosslinking Mechanisms for Programming Reconfigurable Hydrogels Based on Aminopolysaccharides. *Chem. Mater.* **2018**, *30*, 8597−8605.

(13) Yan, K.; Xu, F.; Wang, C.; Li, Y.; Chen, Y.; Li, X.; Lu, Z.; Wang, D. A Multifunctional Metal-Biopolymer Coordinated Double Network Hydrogel Combined with Multi-Stimulus Responsiveness, Self-Healing, Shape Memory and Antibacterial Properties. *Biomater. Sci.* **2020**, *8*, 3193−3201.

(14) Yan, K.; Xu, F.; Li, S.; Li, Y.; Chen, Y.; Wang, D. Ice-Templating of Chitosan/Agarose Porous Composite Hydrogel with Adjustable Water-Sensitive Shape Memory Property and Multi-Staged Degradation Performance. *Colloids Surf., B* **2020**, *190*, No. 110907.

(15) Yan, K.; Xu, F.; Yang, C.; Wei, W.; Chen, Y.; Li, X.; Lu, Z.; Wang, D. Interpenetrating Polysaccharide-Based Hydrogel: A Dynamically Responsive Versatile Medium for Precisely Controlled Synthesis of Nanometals. *Mater. Sci. Eng., C* **2021**, *127*, No. 112211.
(16) Wu, S.; Yan, K.; Zhao, Y.; Tsai, C. C.; Shen, J.; Bentley, W. E.; Chen, Y.; Deng, H.; Du, Y.; Payne, G. F.; Shi, X. Electrical Writing onto a Dynamically Responsive Polysaccharide Medium: Patterning Structure and Function into a Reconfigurable Medium. *Adv. Funct. Mater.* **2018**, *28*, No. 1803139.
(17) Wu, S.; Zhao, Z.; Rzasa, J. R.; Kim, E.; Li, J.; VanArsdale, E.; Bentley, W. E.; Shi, X.; Payne, G. F. Hydrogel Patterning with Catechol Enables Networked Electron Flow. *Adv. Funct. Mater.* **2021**, *31*, No. 2007709.
(18) Zhu, X.; Wu, S.; Yang, C.; Deng, H.; Du, Y.; Shi, X. Electrical Writing to Three-Dimensional Pattern Dynamic Polysaccharide Hydrogel for Programmable Shape Deformation. *Macromol. Rapid Commun.* **2021**, *42*, No. 2000342.
(19) Wu, L.-Q.; Ghodssi, R.; Elabd, Y. A.; Payne, G. F. Biomimetic Pattern Transfer. *Adv. Funct. Mater.* **2005**, *15*, 189−195.
(20) Wu, L.-Q.; McDermott, M. K.; Zhu, C.; Ghodssi, R.; Payne, G. F. Mimicking Biological Phenol Reaction Cascades to Confer Mechanical Function. *Adv. Funct. Mater.* **2006**, *16*, 1967−1974.
(21) Bittner, S. When Quinones Meet Amino Acids: Chemical, Physical and Biological Consequences. *Amino Acids* **2006**, *30*, 205−224.
(22) Hong, M. S.; Choi, G. M.; Kim, J.; Jang, J.; Choi, B.; Kim, J. K.; Jeong, S.; Leem, S.; Kwon, H. Y.; Hwang, H. B.; Im, H. G.; Park, J. U.; Bae, B. S.; Jin, J. Biomimetic Chitin−Silk Hybrids: An Optically Transparent Structural Platform for Wearable Devices and Advanced Electronics. *Adv. Funct. Mater.* **2018**, *28*, No. 1705480.
(23) Ryu, J. H.; Hong, S.; Lee, H. Bio-Inspired Adhesive Catechol-Conjugated Chitosan for Biomedical Applications: A Mini Review. *Acta Biomater.* **2015**, *27*, 101−115.
(24) Faure, E.; Falentin-Daudré, C.; Jérôme, C.; Lyskawa, J.; Fournier, D.; Woisel, P.; Detrembleur, C. Catechols as Versatile Platforms in Polymer Chemistry. *Prog. Polym. Sci.* **2013**, *38*, 236−270.
(25) Wu, S.; Kim, E.; Chen, C. y.; Li, J.; VanArsdale, E.; Grieco, C.; Kohler, B.; Bentley, W. E.; Shi, X.; Payne, G. F. Catechol-Based Molecular Memory Film for Redox Linked Bioelectronics. *Adv. Electron. Mater.* **2020**, *6*, No. 2000452.
(26) Vanarsdale, E.; Hörnström, D.; Sjöberg, G.; Järbur, I.; Pitzer, J.; Payne, G. F.; Van Maris, A. J. A.; Bentley, W. E. A Coculture Based Tyrosine-Tyrosinase Electrochemical Gene Circuit for Connecting Cellular Communication with Electronic Networks. *ACS Synth. Biol.* **2020**, *9*, 1117−1128.
(27) Liu, Y.; Kim, E.; White, I. M.; Bentley, W. E.; Payne, G. F. Information Processing through a Bio-Based Redox Capacitor: Signatures for Redox-Cycling. *Bioelectrochemistry* **2014**, *98*, 94−102.
(28) Kim, E.; Liu, Z.; Liu, Y.; Bentley, W. E.; Payne, G. F. Catechol-Based Hydrogel for Chemical Information Processing. *Biomimetics* **2017**, *2*, No. 11.
(29) Wu, S.; Kim, E.; Li, J.; Bentley, W. E.; Shi, X.-W.; Payne, G. F. Catechol-Based Capacitor for Redox-Linked Bioelectronics. *ACS Appl. Electron. Mater.* **2019**, *1*, 1337−1347.
(30) Kim, E.; Liu, Y.; Shi, X. W.; Yang, X.; Bentley, W. E.; Payne, G. F. Biomimetic Approach to Confer Redox Activity to Thin Chitosan Films. *Adv. Funct. Mater.* **2010**, *20*, 2683−2694.
(31) Kim, E.; Liu, Y.; Bentley, W. E.; Payne, G. F. Redox Capacitor to Establish Bio-Device Redox-Connectivity. *Adv. Funct. Mater.* **2012**, *22*, 1409−1416.
(32) Li, J.; Wu, S.; Kim, E.; Yan, K.; Liu, H.; Liu, C.; Dong, H.; Qu, X.; Shi, X.; Shen, J.; Bentley, W. E.; Payne, G. F. Electrobiofabrication: Electrically Based Fabrication with Biologically Derived Materials. *Biofabrication* **2019**, *11*, No. 032002.
(33) Liu, Y.; Javvaji, V.; Raghavan, S. R.; Bentley, W. E.; Payne, G. F. Glucose Oxidase-Mediated Gelation: A Simple Test to Detect Glucose in Food Products. *J. Agric. Food Chem.* **2012**, *60*, 8963−8967.
(34) Li, Y.; Sun, J.; Mao, W.; Tang, S.; Liu, K.; Qi, T.; Deng, H.; Shen, W.; Chen, L.; Peng, L. Antimony-Doped Tin Oxide Nanoparticles as Peroxidase Mimics for Paper-Based Colorimetric Detection of Glucose Using Smartphone Read-Out. *Microchim. Acta* **2019**, *186*, No. 403.
(35) Aguirre, M. Á.; Long, K. D.; Canals, A.; Cunningham, B. T. Point-of-Use Detection of Ascorbic Acid Using a Spectrometric Smartphone-Based System. *Food Chem.* **2019**, *272*, 141−147.
(36) He, Y.; Zheng, L. Gold Nanoparticle-Catalyzed Clock Reaction of Methylene Blue and Hydrazine for Visual Chronometric Detection of Glutathione and Cysteine. *ACS Sustainable Chem. Eng.* **2017**, *5*, 9355−9359.
(37) Kabir, E.; Kumar, V.; Kim, K. H.; Yip, A. C. K.; Sohn, J. R. Environmental Impacts of Nanomaterials. *J. Environ. Manage.* **2018**, *225*, 261−271.
(38) Liba, B. D.; Kim, E.; Martin, A. N.; Liu, Y.; Bentley, W. E.; Payne, G. F. Biofabricated Film with Enzymatic and Redox-Capacitor Functionalities to Harvest and Store Electrons. *Biofabrication* **2013**, *5*, No. 015008.
(39) Wu, Q.; Wang, L.; Yu, H.; Wang, J.; Chen, Z. Organization of Glucose-Responsive Systems and Their Properties. *Chem. Rev.* **2011**, *111*, 7855−7875.
(40) Meyer, W.; Liu, Y.; Shi, X.-W.; Yang, X.; Bentley, W.; Payne, G. Chitosan-Coated Wires: Conferring Electrical Properties to Chitosan Fibers. *Biomacromolecules* **2009**, *10*, 858−864.
(41) Newman, J. D.; Turner, A. P. F. Home Blood Glucose Biosensors: A Commercial Perspective. *Biosens. Bioelectron.* **2005**, *20*, 2435−2453.
(42) Heller, A.; Feldman, B. Electrochemistry in Diabetes Management. *Acc. Chem. Res.* **2010**, *43*, 963−973.
(43) Heller, A.; Fedman, B. Electrochemical Glucose Sensors and Their Application in Diabetes Management. In *Modern Aspects of Electrochemistry*; Springer, 2013; Vol. *56*, pp 121−187.
(44) Vashist, S. K.; Zheng, D.; Al-Rubeaan, K.; Luong, J. H. T.; Sheu, F. S. Technology behind Commercial Devices for Blood Glucose Monitoring in Diabetes Management: A Review. *Anal. Chim. Acta* **2011**, *703*, 124−136.
(45) Yan, K.; Xiong, Y.; Wu, S.; Bentley, W. E.; Deng, H.; Du, Y.; Payne, G. F.; Shi, X. W. Electro-Molecular Assembly: Electrical Writing of Information into an Erasable Polysaccharide Medium. *ACS Appl. Mater. Interfaces* **2016**, *8*, 19780−19786.
(46) Wu, S.; Yan, K.; Li, J.; Huynh, R. N.; Raub, C. B.; Shen, J.; Shi, X.; Payne, G. F. Electrical Cuing of Chitosan's Mesoscale Organization. *React. Funct. Polym.* **2020**, *148*, No. 104492.
(47) Ozawa, F.; Ino, K.; Takahashi, Y.; Shiku, H.; Matsue, T. Electrodeposition of Alginate Gels for Construction of Vascular-like Structures. *J. Biosci. Bioeng.* **2013**, *115*, 459−461.
(48) Ozawa, F.; Ino, K.; Shiku, H.; Matsue, T. Electrochemical Hydrogel Lithography of Calcium-Alginate Hydrogels for Cell Culture. *Materials* **2016**, *9*, No. 744.
(49) Ozawa, F.; Ino, K.; Arai, T.; Ramón-Azcón, J.; Takahashi, Y.; Shiku, H.; Matsue, T. Alginate Gel Microwell Arrays Using Electrodeposition for Three-Dimensional Cell Culture. *Lab Chip* **2013**, *13*, 3128−3135.
(50) Ino, K.; Ozawa, F.; Dang, N.; Hiramoto, K.; Hino, S.; Akasaka, R.; Nashimoto, Y.; Shiku, H. Biofabrication Using Electrochemical Devices and Systems. *Adv. Biosyst.* **2020**, *4*, No. 1900234.
(51) Cross, E. R. The Electrochemical Fabrication of Hydrogels: A Short Review. *SN Appl. Sci.* **2020**, *2*, No. 397.
(52) Hosu, O.; Ravalli, A.; Lo Piccolo, G. M.; Cristea, C.; Sandulescu, R.; Marrazza, G. Smartphone-Based Immunosensor for CA125 Detection. *Talanta* **2017**, *166*, 234−240.
(53) Wu, J.; Zeng, L.; Li, N.; Liu, C.; Chen, J. A Wash-Free and Label-Free Colorimetric Biosensor for Naked-Eye Detection of Aflatoxin B1 Using G-Quadruplex as the Signal Reporter. *Food Chem.* **2019**, *298*, No. 125034.
(54) Yan, K.; Liu, Y.; Zhang, J.; Correa, S. O.; Shang, W.; Tsai, C. C.; Bentley, W. E.; Shen, J.; Scarcelli, G.; Raub, C. B.; Shi, X. W.; Payne, G. F. Electrical Programming of Soft Matter: Using Temporally Varying Electrical Inputs to Spatially Control Self Assembly. *Biomacromolecules* **2018**, *19*, 364−373.

https://doi.org/10.1021/acssuschemeng.1c04896
ACS Sustainable Chem. Eng. 2021, 9, 14836−14845

(55) Yan, K.; Liu, Y.; Guan, Y.; Bhokisham, N.; Tsao, C. Y.; Kim, E.; Shi, X. W.; Wang, Q.; Bentley, W. E.; Payne, G. F. Catechol-Chitosan Redox Capacitor for Added Amplification in Electrochemical Immunoanalysis. *Colloids Surf., B* **2018**, *169*, 470−477.
(56) Wen, H.; Li, J.; Payne, G. F.; Feng, Q.; Liang, M.; Chen, J.; Dong, H.; Cao, X. Hierarchical Patterning via Dynamic Sacrificial Printing of Stimuli-Responsive Hydrogels. *Biofabrication* **2020**, *12*, No. 035007.
(57) Ouyang, J.; Pu, S.; Chen, X.; Yang, C.; Zhang, X.; Li, D. A Convenient and Rapid Method for Detecting D-Glucose in Honey Used Smartphone. *Food Chem.* **2020**, *331*, No. 127348.
(58) Yang, J.; Hu, X.; Xu, J.; Liu, X.; Yang, L. Single-Step in Situ Acetylcholinesterase-Mediated Alginate Hydrogelation for Enzyme Encapsulation in CE. *Anal. Chem.* **2018**, *90*, 4071−4078.
(59) Xu, J.; Hu, X.; Khan, H.; Tian, M.; Yang, L. Converting Solution Viscosity to Distance-Readout on Paper Substrates Based on Enzyme-Mediated Alginate Hydrogelation: Quantitative Determination of Organophosphorus Pesticides. *Anal. Chim. Acta* **2019**, *1071*, 1−7.
(60) Liu, H.; Qu, X.; Kim, E.; Lei, M.; Dai, K.; Tan, X.; Xu, M.; Li, J.; Liu, Y.; Shi, X.; Li, P.; Payne, G. F.; Liu, C. Bio-Inspired Redox-Cycling Antimicrobial Film for Sustained Generation of Reactive Oxygen Species. *Biomaterials* **2018**, *162*, 109−122.
(61) Kim, E.; Li, J.; Kang, M.; Kelly, D. L.; Chen, S.; Napolitano, A.; Panzella, L.; Shi, X.; Yan, K.; Wu, S.; Shen, J.; Bentley, W. E.; Payne, G. F. Redox Is a Global Biodevice Information Processing Modality. *Proc. IEEE* **2019**, *107*, 1402−1424.

https://doi.org/10.1021/acssuschemeng.1c04896
ACS Sustainable Chem. Eng. 2021, 9, 14836−14845